Investigation of primary cosmic ray spectrum shape by means of EAS muon density technique

I.I. Yashin, A.G. Bogdanov, D.V. Chernov, D.M. Gromushkin, R.P. Kokoulin, G. Mannocchi, A.A. Petrukhin, O. Saavedra, V.V. Shutenko, G. Trinchero

***Abstract*—Results of the study of primary cosmic ray flux features in the energy range 10^{15} – 10^{18} eV by means of the spectra of local density of muons at Experimental complex NEVOD-DECOR are presented. Experimental distributions and spectra obtained on the basis of muon LDFs calculated with CORSIKA code are compared. Possibilities of a new technique of event analysis based on the estimator of effective primary energy for CR flux characteristics study are discussed.**

1. Introduction

At energies above 10^{15} eV, the only source of information on primary cosmic rays and their interactions are extensive air showers (EAS) detected at the Earth surface. A quantitative interpretation of observational results is model dependent and EAS analysis involves many unknown functions: primary CR energy spectrum and composition, extrapolation of hadronic interaction description into UHE and EHE region, and others. As a result, in spite of significant efforts to solve many puzzles of primary CR spectrum (slope, composition, "knee", "second knee", "ankle", GZK cutoff, etc.) there are many questions open till now. Therefore, any new approach to the analysis of detected EAS components together with data on other EAS observables allows to put new constraints on combinations of spectrum, composition and interaction models. Such an approach for investigations of UHE cosmic rays in very wide primary energy range from 10^{15} to 10^{19} eV based on the ground-level measurements of the spectra of local density of EAS muons at various zenith angles was proposed and developed recently [1 - 3].

At large zenith angles, the transverse area of the showers (mainly muons at ground level) generated by UHE primary particles exceeds square kilometers. Hence, muon detector may be considered as a point-like probe and capability of UHE primary particles detection is determined not by size of the setup but by effective EAS dimensions in a plane orthogonal to the shower axis. In this case the observed muon bundle multiplicity m is related to the local muon density D (measured in particles/m^2) as $D \sim m/S_{det}$. Contribution to the flux of events with a fixed local density is given by the showers with different primary energies detected at different distances from the axis; however, due to a fast decrease of cosmic ray flux with the increase of energy, the effective interval of primary particle energies appears relatively narrow [2]. Fixed muon densities at different zenith angles correspond to substantially different primary energies; at that, event collection area increases with zenith angle. It provides a unique possibility to study CR characteristics in a very wide range of primary energies.

Without taking into account fluctuations of the shower development, the integral spectrum of the events in local muon density may be written as:

$$F(\geq D) = \int_0^\infty N(\geq E(\vec{r}, D))dS, \qquad (1)$$

where $\vec{r}$ is the point in the transverse section of the shower, $N(\geq E)$ is the integral primary energy spectrum, and the minimal primary energy E is defined by the equation $\rho(E, \vec{r}) = D$, where $\rho(E, \vec{r})$ is muon LDF in a plane orthogonal to the shower axis. Differential spectrum can be obtained as derivative of expression (1):

$$dF/dD = \int (dN/dE)dS / \left[d\rho(E, \vec{r})/dE \right] . \qquad (2)$$

Preliminary analysis of local muon density spectra (LMDS) characteristics [1 - 3] has shown that spectra exhibit a power type behavior with index β somewhat steeper than that of primary particles ($\beta = \gamma/\kappa \sim 2$; $\kappa \sim 0.9$). Similar to the spectrum of EAS in the total number of muons N_μ, it increases in absolute intensity for heavier nuclei. Selection of the events by muon density enhances the sensitivity to the central part of the shower, therefore the measured distribution is sensitive to primary CR composition and to the features of VHE hadron-nucleus interaction, especially in the forward kinematical region.

In the present paper, the results of the analysis of experimental data on muon bundles detected by means of the NEVOD-DECOR complex on the basis of a new phenomenological EAS observable - local muon density spectra - are described. Experimental spectra of local muon density are compared with expected distributions obtained with the CORSIKA code for certain models of spectrum, composition and hadron interaction. A special attention is paid to the behavior of LMDS in those regions of muon density and zenith angles for generation of which primary particles with

I.I. Yashin, A.G. Bogdanov, D.V. Chernov, D.M. Gromushkin, R.P.Kokoulin, A.A. Petrukhin and V.V. Shutenko are with Moscow Engineering Physics Institute (MEPhI), 115409, Moscow, Russia. E-mail: IIYashin@mephi.ru

G. Mannocchi and G. Trinchero are with Istituto di Fisica dello Spazio Interplanetario, INAF, 10133, Torino, Italy

O. Saavedra is with Dipartimento di Fisica Generale dell Universita di Torino, 10125, Torino, Italy.

energies in the ranges 10^{15} - 10^{16} eV (spectrum “knee”) and around 10^{17} eV (second “knee”) are responsible.

2. Experimental

Experimental local muon density spectra were obtained on the basis of the data on muon bundles accumulated during experimental runs with the NEVOD-DECOR complex in 2002 – 2007 (Fig. 1). The coordinate detector DECOR [4] represents a modular multi-layer system of plastic streamer tube chambers with two-coordinate external strip readout, arranged around the Cherenkov water calorimeter NEVOD with volume 2000 m^3 [5].

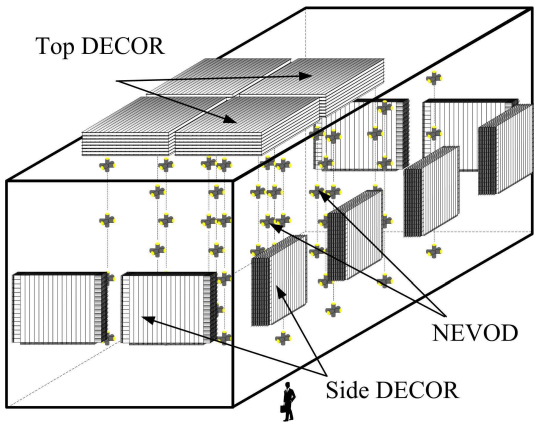

Fig. 1: General layout of NEVOD-DECOR complex.

The side part of DECOR includes eight 8-layer assemblies (supermodules, SM) of chambers with total sensitive area 70 m^2. Angular accuracy of reconstruction of muon tracks crossing the SM is better than 0.7° and 0.8° for projected zenith and azimuth angles, respectively. At large zenith angles, the EAS reach the setup practically as pure muon component. In these conditions muon bundle events have a very bright signature, and their interpretation is unambiguous (Fig. 2). To suppress the residual soft EAS component, for zenith angles < 75° only events in limited intervals of azimuth angle (with DECOR SMs shielded by the water tank) are selected.

It gave possibility to select muon bundles starting from 30° and from a minimal multiplicity determined by trigger conditions ($m \geq 3$).

TABLE I
STATISTICS OF MUON BUNDLE EVENTS

m	θ°	φ°	Live time, h	No. events
≥ 3	30 - 60	120 ≤ φ < 160; 200 ≤ φ < 240	758	18137
≥ 5	30 - 60	120 ≤ φ < 160; 200 ≤ φ < 240	1296	8864
≥ 10	30 - 60	120 ≤ φ < 160; 200 ≤ φ < 240	2680	3272
≥ 3	≥ 60	120 ≤ φ < 160; 200 ≤ φ < 240	1552	4109
≥ 5	≥ 60	120 ≤ φ < 160; 200 ≤ φ < 240	10102	6786
≥ 10	≥ 60	120 ≤ φ < 160; 200 ≤ φ < 240	19922	2013
≥ 10	≥ 75	0 ≤ φ < 360	19922	395

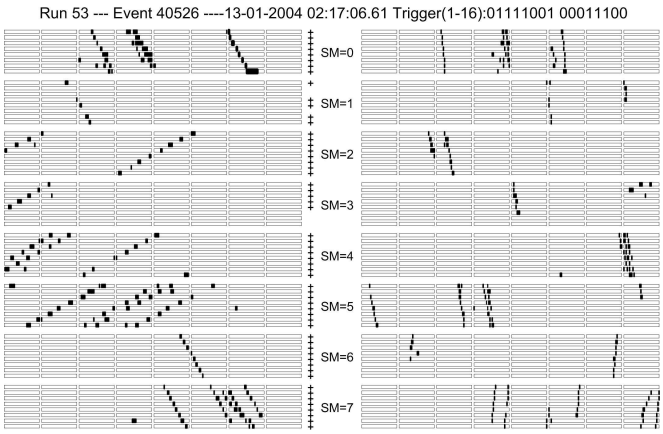

Fig. 2: Example of muon bundle event in the coordinate detector (19 quasi-parallel tracks, 86° zenith angle). Dark points represent hit strips. Left: Y - coordinate (azimuth angle measurements); right: X-coordinate (projected zenith angle)

The event selection procedure includes several stages: trigger selection; soft program selection; scanning of muon bundle candidates, final event classification, and track counting by operators. More detailed description is presented in [1 - 3]. Selection of event was conducted separately for different ranges of θ и m (see Table 1).

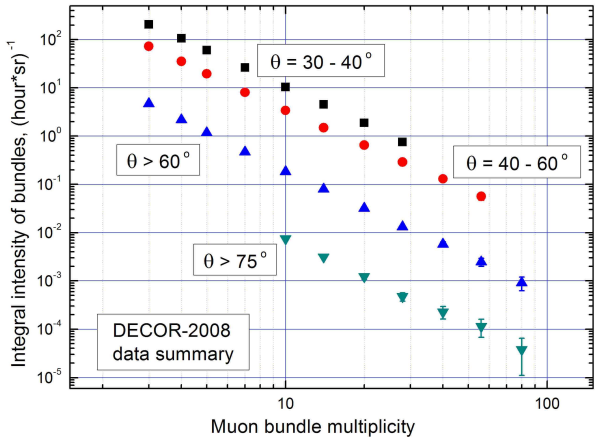

Fig. 3: Integral distributions in muon bundle multiplicity for different zenith angle intervals.

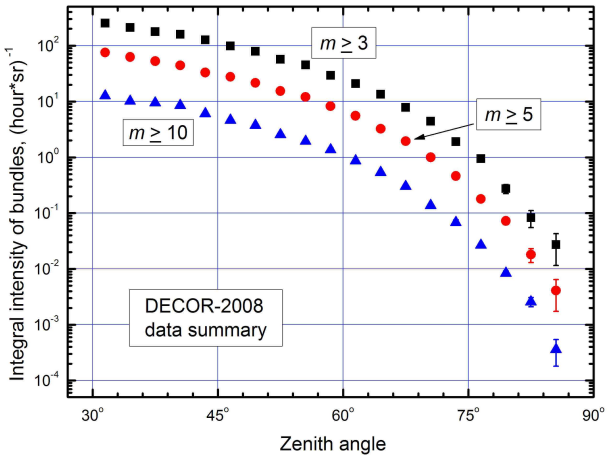

Fig. 4: Distributions in zenith angle for different minimal muon bundle multiplicity

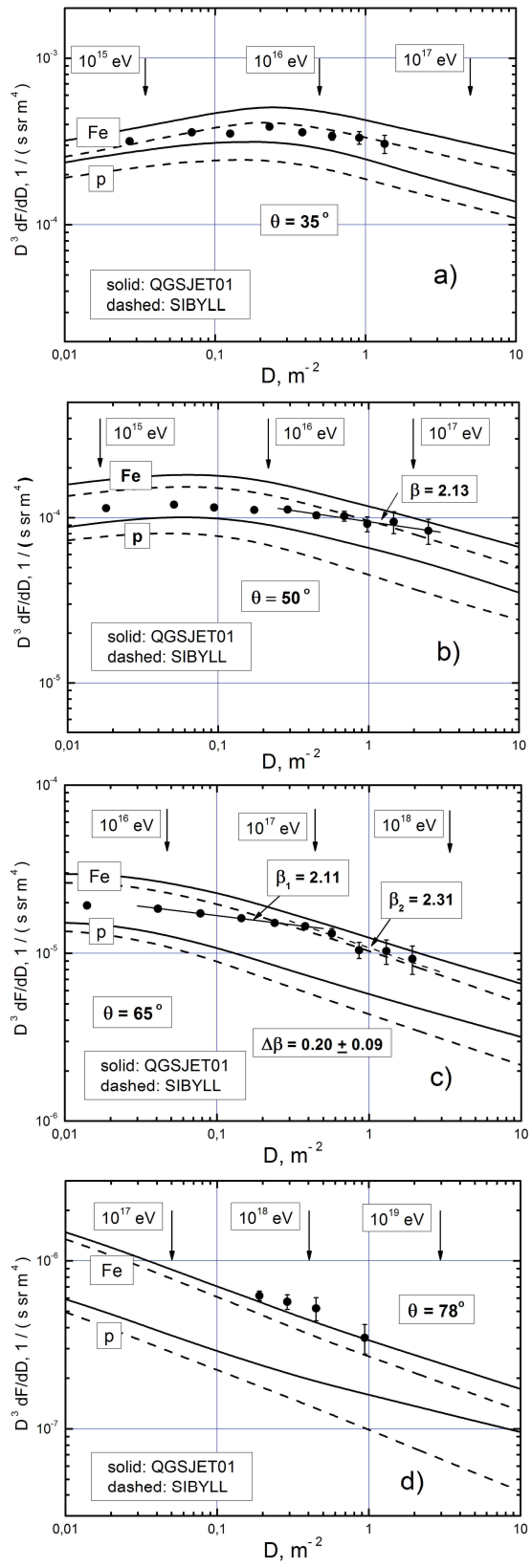

Fig. 5. LMDS for different zenith angles. Points - DECOR data; curves - calculations. a) θ = 35°; b) θ = 50°; thin line represents partial fit of the data between 10^{16} and 10^{17} eV; c) θ = 65°; two lines represent partial fits of the data below and above 10^{17} eV; d) θ = 78°

Muon bundles selected in different zenith angle and multiplicity intervals correspond to different ranges of primary energy. In Fig. 3, the integral distribution in muon bundle multiplicity for different zenith angle intervals is shown. The distributions in zenith angle for different minimal muon bundle multiplicities is presented in Fig. 4. As a whole, experimental muon bundle data cover about 6 – 7 decades in the event intensity.

Reconstruction of LMDS from the observed characteristics of muon bundles represents iterative deconvolution of the measured distributions to detector-independent spectra of local muon density for several zenith angle intervals and is started from estimation of parameters of a spectrum model in a following semi-empirical form:

$$dF_0(D,\theta)/dD = C \cdot D^{-(\beta+1)} \cos^{\alpha}\theta, \qquad (3)$$

where α ~ (4.5 - 4.8) was found from the fit of LMDS distributions in zenith angles by power law function of cosθ. In more detail, the procedure of experimental estimation of LMDS is described in [1].

3. Local density spectra of EAS muons

The measured and calculated differential LMDS multiplied by D^3 for zenith angles 35°, 50°, 65° and 78° are presented in Fig. 5. The points are obtained from different sub-sets of the experimental data summarized in Table 1.

The curves correspond to results of calculations of LMDS on the basis of two dimensional muon LDFs simulated by means of CORSIKA code (v. 6.500 and 6.600) [6] for fixed zenith angles, a set of primary energies (from 10^{14} to 10^{19} eV, one point per decade), pure protons and pure iron nuclei as primary particles, and two combinations of hadron interaction models: QGSJET01c + GHEISHA2002 and SIBYLL2.1 + FLUKA2003.1b. Calculations have been performed with consideration of the Earth magnetic field, which significantly decreases muon density in the central part of the shower [7] and influences the intensity of events selected by muon density [8]. As a reference model of the primary flux, a power type all-particle differential spectrum in the form $dN/dE = 5.0 \times (E, \text{GeV})^{-2.7}$ cm^{-2} s^{-1} sr^{-1} GeV^{-1} below the knee energy, steepening to $(\gamma + 1) = 3.1$ above the knee (4 PeV) was used. This spectrum is close to MSU data as given in [9] and is not much different from other experimental data around the knee. Arrows in the upper part of the figures indicate estimated log-average primary energies responsible for generation of muon bundles with given densities; these estimates only slightly depend on primary particle type and interaction model.

At moderate zenith angles (35°, Fig. 5a), the steepening of the spectra related with the knee is seen both in data and calculations; a reasonable agreement (including the absolute normalisation) of DECOR data with CORSIKA-based simulation is observed. Data for 65° (see Fig. 5c) correspond to intermediate primary energies (about 3 – 500 PeV). In this angular interval, the behavior of experimental LMDS demonstrates a trend to a heavier composition and a hint for an increase of the slope near 10^{17} eV: partial fits of the data above and below this energy (thin lines in the figure) give $\Delta\beta = 0.20 \pm 0.10$. Fit of the “tail” of the experimental spectrum for 50°

has practically the same slope (see Fig. 5b) as the part of the spectrum for 65° before the second knee. It allows to exclude the version about systematical origin of the second knee of local density spectrum. Large multiplicity events in the last angular interval ($m \geq 10$, $\theta > 75°$) correspond to energies around 10^{18} eV (see Fig. 5d). Experimental LMDS qualitatively agree with the expected distributions, but in absolute intensity they are near the limit of the curves calculated on the basis of QGSJET model for iron nuclei.

4. Combined estimator of primary energy

The preceding analysis was based on LMDS obtained in relatively wide bands of zenith angle. However, the effective energy of primary particles strongly depends on zenith angle. To enhance the sensitivity to the shape of primary CR spectrum (first of all, to verify the existence of the "second knee") an event-by-event analysis on the basis of a combined estimator (muon density and zenith angle) of primary particle energy E_{EST} was performed.

In Fig. 6, results of calculations of the average logarithms of the energy of primary particles that give contribution to events with a given local muon density D for several zenith angles (labels near the curves) are presented. The polygons in the figure outline the regions corresponding to selection of muon bundles of different categories. The lower limit of accessible primary energies corresponds to about 10^{15} eV and is determined by low muon densities in such EAS.

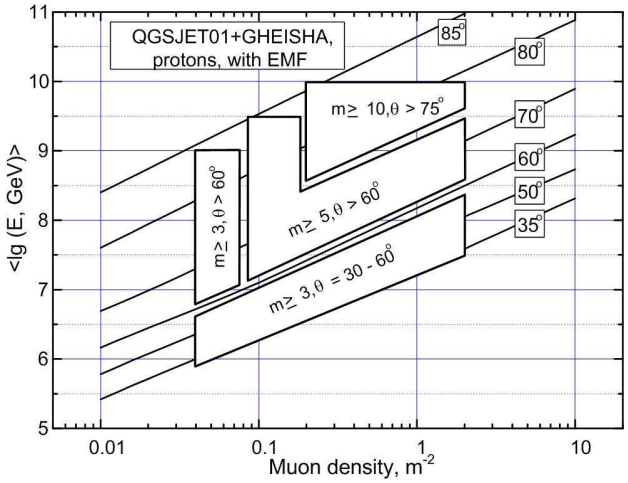

Fig. 6: Average logarithms of primary energies responsible for events with a given local muon density for various zenith angles (see the text)

On the other hand, statistical limitations appear around 10^{19} eV, since the flux of events with such primary energies becomes low. As it follows from Fig. 6, for every event with some set of observables (m, θ, φ) it is possible to attribute a certain effective primary energy.

Results of calculations of <lg(E, GeV)> for primary protons (in frame of above assumptions about energy spectrum and QGSJET01 model) are presented in Figures 7 and 8 as functions of lg$D$ and lg(cosθ). In certain ranges of densities (0.05 - 2.0 m^{-2}), zenith angles (40 - 80°) and primary energies (10^{16} - 10^{18} eV) the dependences in Figures 7 and 8 are well approximated by power law functions:

$$(E_{EST}/E_0)=(D/D_0)^{1.07}\cdot(\sec\theta/\sec\theta_0)^{3.8}. \qquad (4)$$

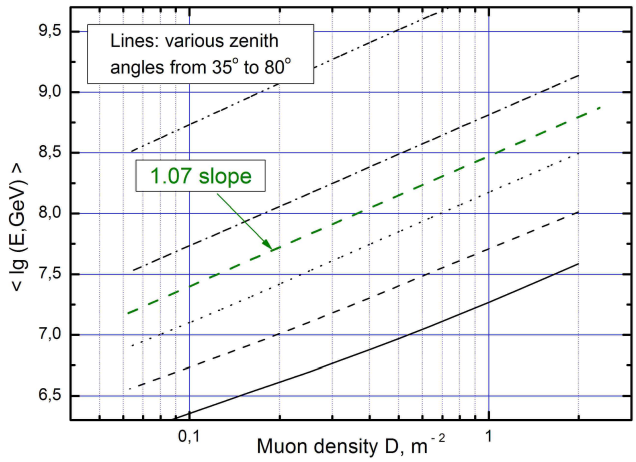

Fig. 7: Dependence of average logarithm of primary energy on lg(D) for different zenith angles

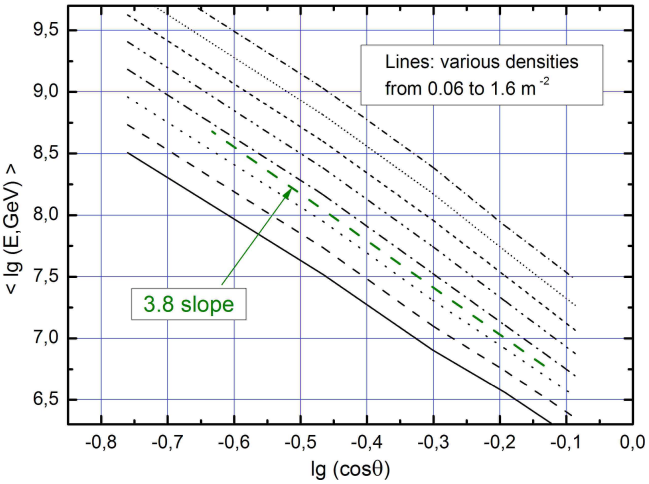

Fig. 8: Dependence of average logarithm of primary energy on lg(cosθ) for different muon densities

Taking as a reference point the energy $E_0 = 10^8$ GeV and zenith angle $\theta_0 = 65°$ we can find (by interpolation of calculated curves) $D_0 = 0.377$ m^{-2}. In this case, the expression (4) for primary energy estimation may be re-written as follows:

$$\lg(E_{EST}, \text{GeV}) = 8.00 + 1.07\,(\lg D + 0.424) - 3.80\,(\lg\cos\theta + 0.374). \qquad (5)$$

This function reproduces calculation data in the above ranges of densities and zenith angles with accuracy better than 2% (in energy), and it is used for event-by-event analysis with primary energy estimator $E_{EST}(m, \theta, \varphi)$. In Figure 9a, experimental and expected distributions of estimates of energy responsible for generation of muon bundles with multiplicities $5 \leq m \leq 55$ and zenith angles $40° \leq \theta \leq 80°$ are presented.

Expected distributions were calculated for a constant index of LMDS $\beta = 2.13$ (without the knee). Experimental distribution is in a good agreement with expected one. The ratio of experimental and calculated distributions is shown in

Figure 9b. A smooth slope variation around $E_{EST} = 10^7$ GeV (close to the first knee) and a hint for increasing of the slope at $E_{EST} > 10^8$ GeV are clearly seen. This ratio was fitted by different power law functions for different intervals of E_{EST}. Fitting results presented in Figure 9b evidence for a gradual increase of the power law index in the given range of E_{EST}. However, it should be noted that the difference of indices obtained around 10^8 GeV ($\Delta\beta = 0.06 \pm 0.04$) is appreciably less than the value obtained as a result of partial fits of differential local muon density spectra for zenith angle 65° ($\Delta\beta = 0.20 \pm 0.10$).

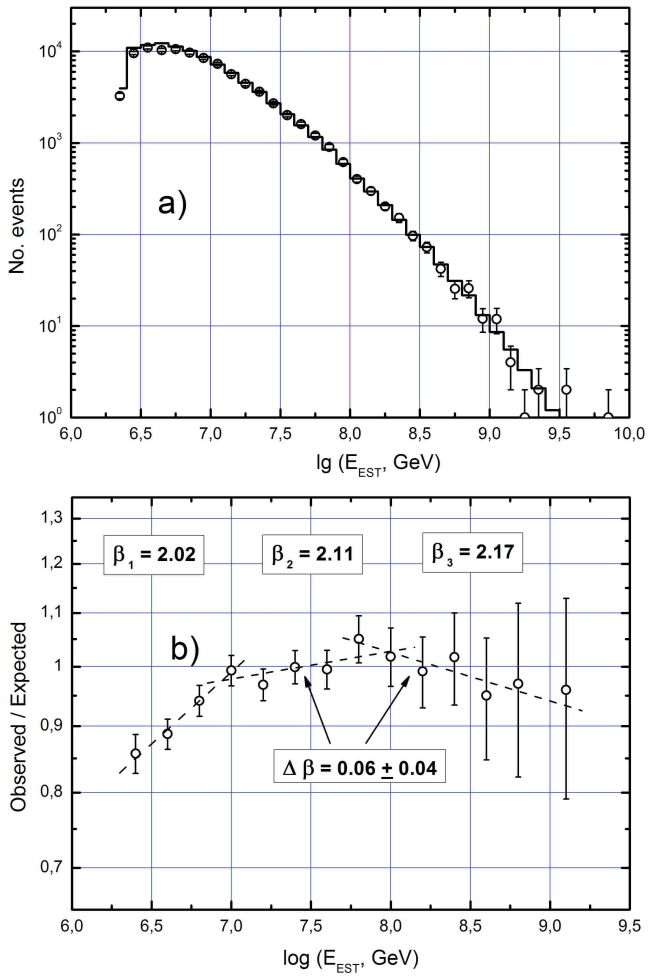

Fig. 9: Experimental and expected distributions of primary energy estimations: a) points – experiment; histogram – calculation ($5 \le m \le 55$ and $40° \le \theta \le 80°$); b) ratio of experimental and expected distributions.

5. Conclusion

Analysis of local muon density spectra for different zenith angles revealed some important features of the spectrum shape: steepening of LMDS related with the knee of primary CR spectrum at PeV energies; a trend to a heavier composition; a hint for an increase of the slope near 10^8 GeV. To obtain additional information about these features, a new technique based on a combined estimator matching a certain muon density and zenith angle with an effective energy of primary particle was applied. This method also reveals the steepening of spectrum around 10^8 GeV but with a smaller change of the slope. As a whole, we can conclude that the comparative analysis of experimental and expected LMDS gives a possibility to study features of spectrum and composition of primary CR and characteristics of hadron interaction in a wide energy range (three decades of primary particles energy) on the basis of a single technique and by means of a single experimental setup.

5. Acknowledgments

The research has been supported by Russian Federal Agency for Education (project RNP.2.1.1.8641), Federal Agency for Science and Innovations (contracts 02.452.11.7064 and NSh-10113.2006.2) and RFBR (grants 07-02-00805-a, 06-02-17000-a, 07-02-13650-ofi-ts).

6. References

[1] N.S. Barbashina et al. “Ultra-high energy cosmic ray investigations by means of EAS muon density measurements”, *Nucl. Phys. B (Proc. Suppl.)*. 165 (2007) 317.

[2] I.I. Yashin et al. “Investigation of muon bundles in horizontal cosmic ray flux”, *Proc. 28th ICRC*, Tsukuba, 3 (2003) 1147.

[3] M.B.Amelchakov et al. “Muon bundles produced by UHE cosmic rays at large zenith angles”, *Physics of Atomic Nuclei*, 70 (2007) 175

[4] M.B. Amelchakov et al. “High-resolution large area coordinate detector for investigations of high energy cosmic ray phenomena at the ground level”, *Proc. 27th ICRC*, Hamburg, 3 (2001) 1267.

[5] V.M. Aynutdinov et al. “Neutrino water detector on the earth's surface (NEVOD)”, *Astrophysics and Space Science*, 258 (1998) 105.

[6] D. Heck et al. http://www-ik.fzk.de/corsika

[7] M. Ave et al. “Modeling horizontal airshowers induced by Cosmic Rays”, *Astropart. Phys.*, 14 (2000) 91.

[8] A.G. Bogdanov et al. “Evidences for the Influence of the Earth's Magnetic Field on EAS Muon Component”, *Proc. 30th ICRC*, Merida, section HE 1.2.A , 4 pp.

[9] S. Eidelman et al. ‘Review of Particle Physics’, *Phys. Lett.*, B592 (2004) 1.